PHYSICAL REVIEW B VOLUME 25, NUMBER 10 15 MAY 1982

Mean-field theory of multilayer physisorption. Adsorbate densities and surface potentials

P. Summerside, E. Sommer,* R. Teshima, and H. J. Kreuzer
Theoretical Physics Institute and Department of Physics, University of Alberta, Edmonton, Alberta T6G 2J1 Canada
(Received 21 October 1981)

Hartree-Fock equations are derived for an inert gas adsorbed on a solid surface for the case of highly mobile physisorption. The temperature and pressure dependence of the coverage is calculated and an effective coverage-dependent surface potential is derived. Single-particle energies and wave functions for adsorbed particles are computed yielding the coverage dependence of the adsorbate density profile and adlayer separations. Gas-solid systems studied numerically are ^{3}He on graphite, ^{4}He on graphite, and Ar on silver.

I. INTRODUCTION

A gas particle is said to physisorb onto the surface of a solid if the net interaction between a gas particle and the solid is accounted for by an effective wall or surface potential $V_s(\vec{r})$, the long-range part of which is essentially the interaction energy between the mutually induced fluctuating dipole moments on the adsorbing gas particle and in the solid. The strong short-range repulsion is largely due to increasing charge fluctuations as the adsorbing particle becomes confined close to the surface. For an inert-gas atom at position $\vec{r}$ in front of a molecular solid, $V_s(\vec{r})$ is well approximated by[1,2]

$$V_s(\vec{r})=\sum_i V(\vec{r}-\vec{r}_i)\ , \tag{1}$$

where $V(\vec{r}-\vec{r}_i)$ is the two-body potential between a gas particle at $\vec{r}$ and a constituent particle of the solid at lattice site $\vec{r}_i$.

The surface potential $V_s(\vec{r})$ will typically develop a number of bound states into which gas particles can be trapped to form the adsorbate. If, due to the structure of the surface crystal plane, $V_s(\vec{r})$ is strongly localized on specific adsorption sites in the surface we speak of localized physisorption. In contrast, for mobile adsorption the surface potential is treated as a function only of the distance z above the uniform surface, $V_s(\vec{r}) \equiv V_s(z)$, so that adsorbed particles can move more or less unhindered along the surface.

At very low (submonolayer) coverages Θ, defined in this regime as the ratio of the number density of adsorbed gas particles per unit surface area to the maximum number density reached upon monolayer completion, we may safely neglect the interactions between the adparticles. However, as Θ approaches unity and the average separation of gas particles in the adsorbate approaches that of a liquid, their mutual interaction potential plays a crucial role in ensuring saturation in a (mobile) fluid adsorbate or causing crystallization in the adsorbed film. Equilibrium theories accounting for these effects have been developed[3,4] in which it is argued that the surface gives rise to an external potential $V_s(\vec{r})$ which provides the basis for establishing a quasi-two-dimensional adsorbed structure. Once reduced to a two-dimensional problem, a virial expansion can be used to include the effects of adparticle-adparticle interactions at low coverage (fluid regime).[3] At near monolayer coverages, strictly two-dimensional lattice models of, for example, the Ising or Potts type can be employed successfully to study phase transitions in films adsorbed on surfaces.[3] The ground-state properties of completed monolayers as well as second- and higher-order layers have been studied by describing the quasi-two-dimensional nature of an adsorbed layer as having a spatial (Gaussian, for example) distribution normal to the surface.[5] In particular, such a distribution makes it possible to account for the anomalously high density in an adsorbed helium monolayer on graphite.

In two-dimensional theories of adsorbed films all coupling associated with energy and particle exchange between the adsorbate and the gas phase is suppressed. This may be quite appropriate for such specific systems as helium adsorbing on grafoil, where the distance between opposing surfaces in grafoil is much shorter than the mean free path of helium away from the surface so that the notion of a gas phase becomes irrelevant. For the

study of adsorption and desorption kinetics at open surfaces, however, the explicit coupling of the adsorbate to the gas phase must form an integral part of the theory. Thus, for example, in the study of adsorption kinetics it is important to know what changing environment additional particles arriving from the gas phase will experience as the coverage on the surface builds up. In a single-particle picture this necessitates the construction of an effective coverage-dependent surface potential given by

$$V_s(\vec{r},\Theta)=V_s(\vec{r})+V_{\mathrm{MF}}(\vec{r},\Theta)\ , \tag{2}$$

where $V_s(\vec{r})$ is the interaction (1) of a single gas particle with the solid, referred to from now on as the bare surface potential. $V_{\mathrm{MF}}(\vec{r},\Theta)$ is the potential arising from the mean field experienced by a gas particle in the presence of all other gas particles already in the surface region at a given coverage Θ. Once this mean-field potential is determined it will be fairly straightforward to extend our quantum-statistical theory of phonon-mediated physisorption[6–10] kinetics to non-negligible coverage. In a quantum-statistical theory the mean-field potential $V_{\mathrm{MF}}(\vec{r},\Theta)$ may be determined by employing temperature-dependent Hartree-Fock theory. Before this can be done two problems have to be considered.

First, the two-body interaction $V_2(\vec{r})$ between the physisorbing (neutral) particles has a strong short-range repulsive singularity so that $V_2(\vec{r})\rightarrow\infty$ as $|\vec{r}|\rightarrow 0$ (for example, as r^{-12} in the Lennard-Jones potential), leading to an infinite Hartree-Fock energy, a difficulty which must be avoided by softening the core of the two-body potential.[11] The second and more subtle problem concerns the fact that the particle density in the adsorbate, say around unit coverage, is of the order of that in liquids, so that the two-body correlations, totally neglected in a straightforward Hartree-Fock theory, become very important. Both of these difficulties may be avoided simultaneously in a systematic way by extending the Hartree-Fock theory to the Brueckner-Hartree-Fock (BHF) theory[11,12] in which the short-range singularity in V_2 is removed by partially including two-body correlations in the construction of a K matrix.

In this paper we will employ the local density approximation to the Brueckner-Hartree-Fock theory. In the next section we review briefly the construction of Brueckner's K matrix as the effective interaction between two fermionic gas particles in the background of a many-body system. The temperature-dependent Brueckner-Hartree-Fock equations are next written down. If we restrict our attention to highly mobile (i.e., fluid) adsorbates, the problem is then reduced to a one-dimensional one so that $V_{\mathrm{MF}}(z,\Theta)$ can be identified as the average Hartree-Fock potential.

In Sec. III we specify the bare surface potential $V_s(z)$ and compute the effective soft core interaction between (fermionic) gas particles starting from Brueckner's K matrix. We will see in the example of ^{3}He that it is the short-range repulsion between ^{3}He particles rather than the quantum (Fermi-Dirac) statistics which determines their two-body correlations and hence gives rise to an effective soft-core potential, so that we can also argue for the usefulness of such a simple (analytic) soft core potential between adsorbing particles obeying Bose-Einstein statistics.

In Sec. IV we outline the method used to cast the Hartree-Fock equations into a set of finite difference matrix equations and discuss the iterative procedure employed to solve them. Section V is then devoted to numerical results. In this paper we present data on temperature-dependent single-particle energies and wave functions of gas particles adsorbing onto a solid surface. We calculate the temperature- and pressure-dependent coverage, the mean position of the adlayers and the effective coverage-dependent surface potential (2). The systems studied here are ^{3}He on graphite, ^{4}He on graphite, and Ar on Ag. Detailed investigation of adsorption isotherms, isosteric heats of adsorption, differential entropies, etc., for these systems is planned to be presented in a second paper of this series, with a third one planned to be devoted to a study of the adsorption and desorption kinetics at non-negligible coverages.

II. THEORY

A. Brueckner-Hartree-Fock theory

The mean-field theory of multilayer physisorption is based on the many-body Hamiltonian

$$\begin{aligned} H&=T+V_s+V_I \\ &=\sum_{i=1}^{N}\frac{p_i^2}{2m}+\sum_{i=1}^{N}V_s(\vec{r}_i) \\ &\quad+\sum_{i<j=1}^{N}V_2(\vec{r}_i-\vec{r}_j)\ , \end{aligned} \tag{3}$$

where T is the kinetic energy of the N gas particles of mass m, V_s is the bare surface potential, and V_I

contains the two-body interactions between gas particles. For neutral atoms or molecules the latter will have a strong repulsive singularity at the origin which, in a Hartree-Fock-type mean-field theory, leads to an infinite contribution to the total energy. This is so because in a mean-field theory all correlations between particles are neglected. In particular, it is the short-range correlations that keep the particles apart and the energy finite. For fermionic gas particles like ^{3}He, Brueckner's theory gives a prescription to partially incorporate two-particle correlations into a mean-field theory by constructing an effective two-body interaction, called the K matrix, which takes the place of V_2 in the Hartree-Fock equations. We will see later on that at typical temperatures and adsorbate densities the theory can also be used in cases where the adsorbing gas particles obey Bose-Einstein statistics, basically because exchange contributions are negligible. This statement is enhanced for heavier gas particles for which the quantum statistics of the particles become even less important. We will therefore continue for now to develop our theory for fermionic gas particles, our prototype system being ^{3}He adsorbing on graphite.

Brueckner's K matrix is defined by[13]

$$V_2\psi = K\Phi \,, \tag{4}$$

where $\Phi(\vec{r}_1,\vec{r}_2)$ is a free two-particle state and $\psi(\vec{r}_1,\vec{r}_2)$ is the fully correlated wave function for two gas particles at positions $\vec{r}_1$ and $\vec{r}_2$, interacting via $V_2(\vec{r}_1,\vec{r}_2)$ in the background of the $(N-2)$ other gas particles. The K matrix satisfies the Brueckner integral equation

$$K = V_2 - V_2 \frac{Q}{e} K \,, \tag{5}$$

Q being the Pauli exclusion operator and

$$e = H^{\mathrm{SCF}} - \omega \,, \tag{6}$$

where H^{SCF} is the Hamiltonian of the self-consistent mean field and ω is called the starting energy. Replacing V_2 in the total Hamiltonian (3) by the K matrix, a variational calculation leads to the spin-averaged temperature-dependent Brueckner-Hartree-Fock equations[14]

$$\left[-\frac{\hbar^2}{2m}\nabla^2_{\vec{r}_1} + V_s(\vec{r}_1) - E_{\vec{i}}\right]\psi_{\vec{i}}(\vec{r}_1) + \sum_{\vec{j}} n_{\vec{j}} \int d\vec{r}_2 d\vec{r}_3 d\vec{r}_4 \psi^*_{\vec{j}}(\vec{r}_2)\langle \vec{r}_1,\vec{r}_2 \mid K \mid \vec{r}_3,\vec{r}_4\rangle$$
$$\times[(2s+1)\psi_{\vec{i}}(\vec{r}_3)\psi_{\vec{j}}(\vec{r}_4) - \psi_{\vec{j}}(\vec{r}_3)\psi_{\vec{i}}(\vec{r}_4)] = 0 \,, \tag{7}$$

where $E_{\vec{i}}$ and $\psi_{\vec{i}}$ are the single-particle energies and wave functions, respectively, and s is the spin. The thermal occupation functions are given by

$$n_{\vec{j}} = [\exp(E_{\vec{j}} - \mu) + 1]^{-1} \tag{8}$$

where μ is the chemical potential per particle. Because we assume that the gas phase is very large (infinite), it controls μ in equilibrium. Thus if away from the surface, the gas can be described satisfactorily by the ideal gas law, then

$$\mu = k_B T \ln \frac{h^3 P}{(2\pi m)^{3/2}(k_B T)^{5/2}} \,, \tag{9}$$

where P is the pressure in the gas phase.

Whereas the inclusion of temperature effects in the Hartree-Fock equations (7) is well understood, no extension of the K matrix theory to nonzero temperatures has been given to our knowledge. At $T=0$ the Pauli exclusion operator Q allows only unoccupied states above the Fermi level to appear as intermediate states in (5). For $T>0$ one might then try to write

$$Q = \sum_i (1 - n_{\vec{i}}) \mid \vec{i}\rangle\langle \vec{i} \mid \,.$$

We will, however, see below after we have invoked several approximations in our theory, that such considerations are less important.

In principle, one now seeks a self-consistent solution to the nonlinear equations (7). However, this requires a knowledge of the K matrix which, in turn, depends on the single-particle energies $E_{\vec{i}}$ through the energy denominator (6). It seems impracticable to deal with this double self-consistency problem numerically, and certain approximations must be invoked as discussed in the next section.

B. Hartree-Fock theory with a local effective interaction

To decouple the Brueckner self-consistency in (5) from the Hartree-Fock self-consistency in (7) one invokes a local density approximation[11,12] whereby Eq. (5) is solved in a fictitious infinite system at the (average) adsorbate density as determined by the solution of (7). Proceeding in the standard way we introduce relative and center of mass coordinates in the K matrix and decompose it into partial wave contributions to obtain[15]

$$\langle \vec{R}_{\alpha\beta} | K | \vec{R}_{\gamma\delta} \rangle = \frac{4\pi}{(2\pi)^3} \sum_l (2l+1) \int_0^\infty k^2 dk \; j_l(kR_{\alpha\beta}) V_2(R_{\gamma\delta}) u_l(k,R_{\gamma\delta}) P_l(\hat{R}_{\alpha\beta}\cdot\hat{R}_{\gamma\delta}) , \tag{10}$$

where $\vec{R}_{\alpha\beta}=\vec{r}_\alpha-\vec{r}_\beta$, $R=|\vec{R}|$, and $\hat{R}=\vec{R}/R$. The Brueckner wave function $u_l(k,R)$ satisfies the integral equation

$$u_l(k,R)=j_l(kR)+\int_0^\infty R'^2 dR' G_l(R,R') V(R') u_l(k,R') \tag{11}$$

with Green's function

$$G_l(R,R')=-\frac{2}{\pi}\int_0^\infty k^2 dk \frac{Q}{e} j_l(kR) j_l(kR') , \tag{12}$$

where j_l is a spherical Bessel function. Equation (11) can be solved in various approximations as discussed in Sec. III A so that (10) can be assumed to be known. It then remains to reduce (7) to a manageable problem, the outstanding difficulty being the appearance of multiple integrations involving the K matrix. Even in the case of highly mobile adsorption, the simplifications afforded by the fact that $V_s(\vec{r})$ reduces to a function of z only are not sufficient to allow a numerical solution of (7).[16] Our task is greatly simplified, however, if we approximate the nonlocal K matrix by a local effective interaction, i.e., by writing

$$\langle \vec{r} | K | \vec{r}' \rangle = V_{\text{eff}}(\vec{r}) \delta(\vec{r}-\vec{r}') , \tag{13}$$

where obviously[12,17]

$$V_{\text{eff}}(\vec{r})=\int \langle \vec{r} | K | \vec{r}' \rangle d\vec{r}' = \frac{2}{\pi}\int_0^\infty r'^2 dr' \int_0^\infty k^2 dk \; \sin(kr) V_2(r') u_0(k,r') . \tag{14}$$

Equations (7) then read

$$\left[-\frac{\hbar^2}{2m}\nabla^2_{\vec{r}}+V_s(\vec{r})-E_{\vec{i}}\right]\psi_{\vec{i}}(\vec{r})+\sum_{\vec{j}} n_{\vec{j}} \int d\vec{r}' \psi^*_{\vec{j}}(\vec{r}') V_{\text{eff}}(\vec{r}-\vec{r}') \times[(2s+1)\psi_{\vec{i}}(\vec{r})\psi_{\vec{j}}(\vec{r}')-\psi_{\vec{j}}(\vec{r}')-\psi_{\vec{j}}(\vec{r})\psi_{\vec{i}}(\vec{r}')]=0 . \tag{15}$$

These are the standard Hartree-Fock equations for particles obeying Fermi-Dirac statistics and interacting via $V_{\text{eff}}(\vec{r})$.

C. Reduction to one dimension for mobile adsorption

Further simplifications in (15) can now be introduced by considering the case of mobile adsorption. We reduce (15) to a one-dimensional problem by considering gas-solid systems with a surface potential

$$V_s(\vec{r})=V_s(z) , \tag{16}$$

depending on the distance from the surface only. The general case where $V_s(\vec{r})$ is periodic along the surface is treated in the Appendix. As long as the adsorbate remains fluid, i.e., does not crystallize into a two-dimensional structure, we can assume that

$$\psi_{\vec{i}}(\vec{r})=L^{-1}\Phi_{\vec{i}}(z)e^{i\vec{q}\cdot\vec{\rho}} , \tag{17}$$

where L^2 is the surface area, $\vec{q}=(q_x,q_y)$ is a two-dimensional wave vector, $\vec{r}=(\vec{\rho},z)$, and $\vec{i}=(q_x,q_y,i)$ with i enumerating the bound states and the continuum. Inserting (17) into (15) and integrating out the lateral degrees of freedom we obtain

$$\left[-\frac{\hbar^2}{2m}\frac{d^2}{dz^2}+V_s(z)-\epsilon_i(\vec{q})\right]\Phi_i(z,\vec{q})+\sum_j \frac{1}{(2\pi)^2}\int d\vec{q}'\left\{\exp\left[\beta\left[\epsilon_j(\vec{q}')+\frac{\hbar^2 q'^2}{2m}-\mu\right]\right]\mp 1\right\}^{-1}$$
$$\times\int dz'\Phi_j^*(z',q')\int d\vec{\rho}\, V_{\rm eff}(z-z',\vec{\rho})[(2s+1)\Phi_i(z,\vec{q})\Phi_j(z',\vec{q}')$$
$$\pm e^{-i(\vec{q}'-\vec{q})\cdot\vec{\rho}}\Phi_i(z',\vec{q})\Phi_j(z,\vec{q}')]=0\ , \tag{18}$$

where

$$\epsilon_i(\vec{q})=E_{\vec{i}}-\frac{\hbar^2 q^2}{2m}\ , \tag{19}$$

and the upper (lower) sign must be used if the gas particles obey Bose-Einstein (Fermi-Dirac) statistics.

The set of coupled nonlinear integro-differential equations (18) determines the single-particle energies $\epsilon_i(\vec{q})$ and wave functions $\Phi_i(z,\vec{q})$ at a given temperature T for each two-dimensional wave vector $\vec{q}$. The latter appears explicitly only in the exponential factor $\exp[i(\vec{q}'-\vec{q})\cdot\vec{\rho}]$ in the exchange term, which if small, would certainly justify the replacement of this exponential factor by unity. The eigenvalues ϵ_i and eigenfunctions Φ_i would then be independent of $\vec{q}$, simplifying the task of solving (18) tremendously. We introduce an approximation to this effect with the following qualitative discussion of (18) and its solutions, anticipating some of the insight we have gained from our numerical work, a detailed discussion of which is given in Sec. V.

At high temperature the system will exhibit low coverage, and the energy of the lowest bound state ϵ_0 will be of the order of the (negative) heat of adsorption, $\epsilon_0\approx -Q$. With μ given by (9) we quantify the term "high temperature" by insisting that $\beta(\epsilon_0-\mu)<<1$. In that case the thermal occupation functions in (18) can be approximated by the classical Maxwell-Boltzmann distribution resulting in a very small factor $\exp(\beta\mu)$ multiplying the Hartree-Fock terms. The gas particles then experience only the bare surface potential $V_s(z)$ with their number density given by

$$\rho(\vec{r})\approx\sum_{\vec{i}}|\psi_{\vec{i}}(\vec{r})|^2 e^{-\beta(E_{\vec{i}}-\mu)}$$
$$\approx\left[1+\frac{\hbar}{(2\pi m k_B T)^{1/2}}\sum_{i\,(\rm BS)} e^{-\beta\epsilon_i}|\Phi_i(z)|^2\right]\rho_0\ , \tag{20}$$

where the sum over i includes bound states (BS) only and ρ_0 is the asymptotic density in the gas phase far away from the solid. As we lower the temperature, quantum statistics become relevant for the bound state occupation functions and (20) reads, using (17),

$$\rho(\vec{r})=\sum_{\vec{i}}|\psi_{\vec{i}}(\vec{r})|^2\{\exp[\beta(E_{\vec{i}}-\mu)]\pm 1\}^{-1}$$
$$=\rho_0+\sum_{i\,(\rm BS)}(2\pi)^{-2}\int d\vec{q}\,|\Phi_i(z,\vec{q})|^2(e^{\beta[\epsilon_i(\vec{q})+\hbar^2q^2/2m-\mu]}\pm 1)^{-1}\ , \tag{21}$$

If the eigenvalues $\epsilon_i(\vec{q})$ of (18) were independent of $\vec{q}$ and T, then the density in the surface region would, upon lowering T and thus raising μ in (9), eventually exceed the density in a liquid and for Bose-Einstein statistics, indeed, approach infinity. Thus the eigenvalues $\epsilon_i(\vec{q})$ must increase as temperature is lowered so that (21) produces the correct adsorbate density. For gas particles obeying Bose-Einstein statistics this implies that $\epsilon_i(\vec{q})\gtrsim\mu$. For fermionic gas particles such an argument would suggest that at low temperatures, as the ith adlayer fills, we have $\epsilon_i(\vec{q})\lesssim\mu$. For either statistics we thus find ϵ_i of the order of μ. If this argument is correct then statistics are not very important and we would expect, for example, ^{3}He and ^{4}He to adsorb in a similar fashion onto a given substrate. This, of course, would also imply that the exchange term in (18) is not very important and approximating the exponential term $\exp[i(\vec{q}'-\vec{q})\cdot\vec{\rho}]$ in it by unity would seem justified. This then decouples the equations (18) in $\vec{q}$, making ϵ_i and Φ_i independent of $\vec{q}$, so that we can finally write for (18)

$$\left[-\frac{\hbar^2}{2m}\frac{d^2}{dz^2}+V_s(z)-\epsilon_i\right]\Phi_i(z)+\sum_j \tilde{n}_j\int dz'\tilde{V}(z-z')\Phi_j^*(z')[(2s+1)\Phi_i(z)\Phi_j(z')\pm\Phi_i(z')\Phi_j(z)]=0\ , \tag{22}$$

where

$$\tilde{n}_j=\frac{\sigma_g^2}{A}\sum_{\vec{q}} n_{\vec{q}j}=(2\pi)^{-1}\sigma_g^2\int q\,dq(e^{\beta[\epsilon_j+(\hbar^2q^2/2m)-\mu]}\mp 1)^{-1}$$

$$=\mp(2\pi)^{-1}mk_BT\sigma_g^2\hbar^{-2}\ln(1\mp e^{-\beta(\epsilon_j-\mu)}) \tag{23}$$

and

$$\tilde{V}(z)=\sigma_g^{-2}\int d\vec{\rho}\,V_{\rm eff}(z,\vec{\rho})\ . \tag{24}$$

The powers of the range σ_g of the two-body interaction $V_{\rm eff}(\vec{r})$ have been introduced so as to render the occupation functions $\tilde{n}_j$ dimensionless and to keep units of energy for the effective one-dimensional potential $\tilde{V}(z)$.

We can now identify the mean-field potential $V_{\rm MF}(z,\theta)$. From (22) we see that it receives one contribution from the Hartree term, namely

$$V_{\rm MF}^{(H)}(z,\Theta)=\sum_j \tilde{n}_j\int dz'\tilde{V}(z-z')\Phi_j^*(z')\Phi_j(z')\ , \tag{25}$$

where the coverage is given by

$$\Theta=\sum_j\Theta_j=\sum_j\tilde{n}_j/\tilde{n}_j^{\max}\ . \tag{26}$$

The contribution of the exchange or Fock term in (22) to the mean-field potential is less straightforward due to its nonlocality and state dependence. One option is to write the Fock term as

$$\left[\sum_j \tilde{n}_j\int dz'\Phi_j^*(z')\Phi_i(z')\Phi_j(z)\Phi_i^{-1}(z)\right]\Phi_i(z) \tag{27}$$

which defines a local, state-dependent potential in the large parentheses. Its usefulness as an intuitive tool is somewhat reduced by the fact that it is singular wherever $\Phi_i(z)$ has a zero. We therefore prefer to include as part of the mean-field potential $V_{\rm MF}(z,\Theta)$ the statistical average of the Fock term,[18]

$$\bar{V}_{\rm MF}^{(F)}=\sum_{k,j}\tilde{n}_k\tilde{n}_j\int dz'\tilde{V}(z-z')\Phi_j^*(z')\Phi_k(z')\Phi_k^*(z)\Phi_j(z')\Big/\sum_l\tilde{n}_l\,|\,\Phi_l(z)\,|^2\ , \tag{28}$$

so that finally

$$V_s(z,\Theta)=V_s(z)+V_{\rm MF}^{(H)}(z,\Theta)+\bar{V}_{\rm MF}^{(F)}(z,\Theta)\ . \tag{29}$$

Numerical examples of this coverage-dependent surface potential will be discussed for various gas-solid systems in Sec. V.

Let us note in closing that for light fermionic gas particles saturation in the adsorbate could also be achieved via the $\vec{q}$ dependence of $\epsilon_j(\vec{q})$ arising from the full exchange term in (18). If at low temperature $\epsilon_j(\vec{q})$ is such that for $q<q_c^{(j)}$, $\epsilon_j(q)\approx\epsilon_j(0)<<\mu$ and for $q>q_c^{(j)}$, $\epsilon_j(q)>>\mu$ then (8) behaves like a zero temperature Fermi-Dirac distribution. Equation (23) then reads

$$\tilde{n}_j\approx\frac{mk_BT}{2\pi\hbar^2}\sigma_g^2\ln[(1+e^{-\beta[\epsilon_j(0)-\mu]})]/[(1+e^{-\beta[\epsilon_j(0)-\mu+(\hbar^2q_c^{(j)2}/2m)]})]\ , \tag{30}$$

which would lead at zero temperature to a two-dimensional number density $q_c^{(j)2}/2\pi$ in the jth adlayer.

III. SURFACE POTENTIAL AND EFFECTIVE TWO-BODY POTENTIAL

Before we can proceed with a numerical solution of the Hartree-Fock equations (22), we must specify the bare surface potential $V_s(z)$ and the effective two-body interaction $\tilde{V}(z)$ for specific gas-solid systems. Starting with $V_s(z)$ we recall Eq. (1) which says that for inert gas atoms like He, Ar, Kr, etc., physisorbing on a molecular solid like graphite $V_s(z)$ is the sum of pairwise Lennard-Jones type interactions. Such potentials have been analyzed in great detail by Steele[1] with more recent investigations particularly of the He-graphite system by Cole and co-workers.[2] If the two-body interaction between a gas particle and a particle of the solid can be adequately described by a Lennard-Jones potential

$$V(r)=4\epsilon_s[(\sigma_s/r)^{12}-(\sigma_s/r)^6] , \tag{31}$$

then for mobile adsorbates, we replace the sum in (1) over atoms in a given crystal plane parallel to the surface by an integration over a uniform plane of the same average atom density and sum this laterally averaged potential over the crystal planes to obtain the ζ potential,

$$V_s(z)= 2\pi\epsilon_s\sigma_s^6 c_s a_s^{-1} d_s^{-4} \times[\tfrac{2}{5}(\sigma_s/d_s)^6\zeta(10,z/d_s)-\zeta(4,z/d_s)] , \tag{32}$$

where

$$\zeta(n,x)=\sum_{j=0}^{\infty}(j+x)^{-n} \tag{33}$$

is a Riemann ζ function. d_s is the distance between crystal planes and $n_s=c_s/a_s$ is the average lateral density of the basal plane whose two-dimensional unit cell of area a_s contains c_s atoms.

Inert-gas atoms physisorbing on metal surfaces interact predominantly with their image dipoles produced as a result of the dielectric response of the conduction electrons, and a collective rather than pairwise summation of the net gas particle-solid interaction is more appropriate. For gas-metal systems with highly mobile physisorbed adsorbates a simple one-dimensional Morse potential,

$$V_s(z)=U_0(e^{-2\gamma_s(z-z_0)}-2e^{-\gamma_s(z-z_0)}) , \tag{34}$$

has been shown to be adequate. We will use both potential models (32) and (34) in our numerical work in Sec. V.

Turning our attention next to the effective two-body interaction (24), we must solve (11) for $l=0$ to determine $V_{\rm eff}(\vec{r})$ in (14). For ^{3}He at liquid densities and at $T=0$ K, (11) has been solved by Østgaard[15] and by Ghassib, Ibarra and Irvine[19] invoking several approximations that had been developed for nuclear matter. In the effective-mass approximation one writes the energy denominator (6) in (12) as

$$e=e(k^2)=\frac{\hbar^2}{mm^*}\left[k^2+2\Delta k_f^2-\frac{m^*}{m_0^*}k_0^2\right] \tag{35}$$

with typical values for the effective masses m^* for $k>k_f$ and m_0^* for $k<k_f$, for the energy gap Δ and the starting momentum k_0 given by Østgaard[15] at typical ^{3}He densities. In evaluating (11) we also used the reference spectrum method which takes $Q=1$, an approximation that has proven very reliable and expedient.[11,15] A numerical example of the effective potential (14) for a Lennard-Jones potential

$$V_2(r)=4\epsilon_g[(\sigma_g/r)^{12}-(\sigma_g/r)^6] \tag{36}$$

is given in Fig. 1(a). Important to note is the fact that the repulsive core in V_2 has been reduced substantially. Because ^{3}He atoms cannot approach each other much closer than σ_g, the short range repulsion for $r<\sigma_g$ should not contribute too much to the ground-state energy as evaluated by a Brueckner-Hartree-Fock theory.

Carrying out the lateral integration of $V_{\rm eff}(r)$ according to (24), we derive from the result depicted in Fig. 1(a) the effective one-dimensional interaction $\tilde{V}(z)$ as shown in Fig. 1(b). Because $\tilde{V}(z)$ represents the effective interaction between two ^{3}He layers of liquid density a distance z apart, it must develop a repulsive barrier for $z<\sigma_g$ so as to prevent these layers from penetrating each other. The height $\tilde{V}(0)$ is found to vary more or less linearly with the lateral density to account for the fact that at higher densities, i.e., at shorter mean separation between the particles, more of the repulsive core contributes to the total energy of the system. In a completely self-consistent Brueckner-Hartree-Fock theory $\tilde{V}(z)$ would have to be determined at each density as calculated from the Hartree-Fock equations (22). Since $\tilde{V}(z)$ changes

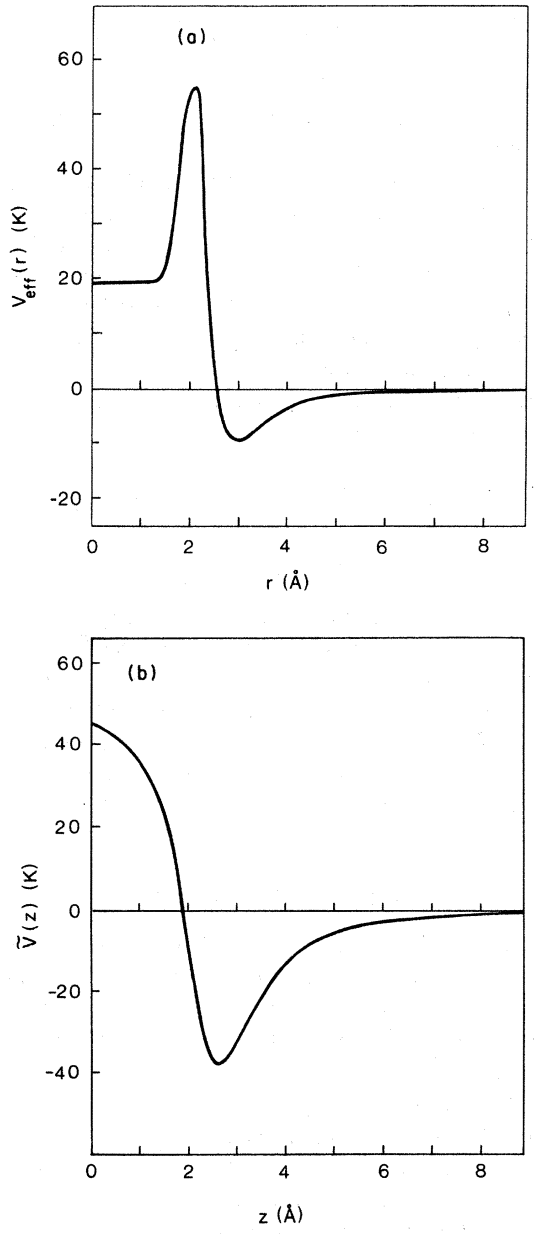

FIG. 1. (a) Effective two-body potential $V_{\rm eff}(r)$ between ^{3}He particles calculated from (14) in the effective mass approximation. Parameters taken from Ref. 15: $m^*=1$, $m_0^*=2.5$, $\Delta=0.4$, $k_f=0.9$ Å^{-1}, $k_0=0.8k_f$, $\epsilon_g/k_B=10.22$ K, $\sigma_g=2.556$ Å. (b) One-dimensional effective two-body potential from (24) integrating $V_{\rm eff}(r)$ above.

little as a function of density apart from the linear dependence of $\tilde{V}(0)$, we prefer here to parametrize $\tilde{V}(z)$ in a reasonable way and keep $\tilde{V}(0)$ as an input parameter. Indeed, it is the only truly free parameter in our theory. To arrive at a suitable algebraic parametrization of $\tilde{V}(z)$ we first note that for $u_0(k,r')=\sin(kr')$ Eq. (14) is trivial, and (24) gives the unscreened two-body interaction in one dimension

$$\tilde{V}^{(0)}(z)=2\pi\epsilon_g[\tfrac{2}{5}(\sigma_g/z)^{10}-(\sigma_g/z)^4]\ . \tag{37}$$

We then parametrize the screening by the short-range correlations which render $\tilde{V}(z=0)$ finite by writing

$$\tilde{V}(z)=2\pi\epsilon_g z^{10} \times\{z^{10}+A\sigma_g^{10}\exp[-(z/z_1)^\alpha]\}^{-1} \times[\tfrac{2}{5}(\sigma_g/z)^{10}-(\sigma_g/z)^4]\ . \tag{38}$$

The parameters z_1 and α are fairly well determined: z_1 is always close to the zero of the unscreened potential $\tilde{V}^{(0)}(z)$, and α is of order 10 to 15 so that the attractive well of (37) is not affected. In the limit $z\to 0$ (38) yields $\tilde{V}(0)=4\pi\epsilon_g/5A$ so that A alone determines the finite barrier height and is thus our only adjustable parameter.

Let us finally note that for ^{3}He below liquid density the reference spectrum method, i.e., setting $Q=1$ in (12), does not change Figs. 1(a) and 1(b) qualitatively. This seems to imply that the two-body correlations incorporated in the K matrix are largely determined by the strong repulsion in V_2 which, however, does not depend on the spin and statistics of the interacting particles. It therefore seems justified to use the phenomenological soft-core potential (38) also for gas particles that obey Bose-Einstein statistics.

IV. NUMERICAL METHOD

To obtain the self-consistent solution to the Hartree-Fock equations (22) numerically, we enclose the system in a finite one-dimensional box of length L and discretize the distance from the surface wall according to $z_n=(n/N_0)L$, $n=0,1,2,\ldots,N_0$. The dimension L of the box must be sufficiently large to allow for the possible development of several adsorbed layers and is thus governed primarily by the range of the two-body potential between the gas particles which plays the dominant role in determining the interlayer spacing. The number of points N_0 and hence the dimension of the matrices involved in the calculation must then be chosen sufficiently large to allow for a precise computation of the wave functions.

The Hartree-Fock equations (22) are cast into a set of finite-difference matrix equations. The dif-

ferential operator is written as a fifth-order difference operator using a five-point Lagrangian interpolation and the spatial integrals are approximated by discrete sums. The resulting matrix equation then reads

$$(\overleftrightarrow{M}_D+\overleftrightarrow{M}_S+\overleftrightarrow{M}_H+\overleftrightarrow{M}_F+\epsilon_i\overleftrightarrow{1})\vec{\Phi}_i=0 \tag{39}$$

where

$$\vec{\Phi}_i=(\Phi_i(z_1),\Phi_i(z_2),\ldots,\Phi_i(z_N)) . \tag{40}$$

The matrices arising from the differential operator, the surface potential, and the Hartree and Fock potentials, respectively, are defined by

$$\left[\frac{2m}{\hbar^2}\right]\left[\frac{L}{N}\right]^2 M_D(z_m,z_n)=-\tfrac{5}{2}\delta_{mn}+\tfrac{4}{3}\delta_{m,n\pm1}-\tfrac{1}{12}\delta_{m,n\pm2} , \tag{41}$$

$$M_S(z_m,z_n)=V_s(z_m)\delta_{mn} , \tag{42}$$

$$M_H(z_m,z_n)=(2s+1)\delta_{mn}\sum_{l=1}^{N}\tilde{V}(|z_m-z_l|)\sum_{j=1}^{N}\tilde{n}_j|\Phi_j(z_l)|^2 , \tag{43}$$

and

$$M_F(z_m,z_n)=\pm(1-\delta_{mn})\tilde{V}(|z_m-z_n|)\sum_{j=1}^{N}\tilde{n}_j\Phi_j(z_m)\Phi_j(z_n) . \tag{44}$$

Here, s is the spin of the gas particles, taken as 0 or $\frac{1}{2}$ with the respective plus or minus sign in (44) for bosons and fermions and the appropriate temperature-dependent occupation functions $\tilde{n}_j$ as given in (23) or (30).

The self-consistent solutions of (39) are found by an iterative procedure. It is initiated at high temperatures where all $\tilde{n}_j$ and thus the Hartree and Fock matrices $\overleftrightarrow{M}_H$ and $\overleftrightarrow{M}_F$ are negligibly small. The eigenvalues ϵ_i and eigenfunctions Φ_i as determined by the surface potential matrix $\overleftrightarrow{M}_S$ alone then provide good estimates to calculate $\overleftrightarrow{M}_H$ and $\overleftrightarrow{M}_F$ for the next diagonalization of the complete matrix equation (39). Before calculating $\overleftrightarrow{M}_H$ and $\overleftrightarrow{M}_F$ for subsequent iterations the following averaging procedure is used:

$$\begin{aligned}\bar{\Phi}^{(n)}&=\lambda\Phi^{(n)}+(1-\lambda)\bar{\Phi}^{(n-1)} ,\\ \bar{\epsilon}^{(n)}&=\lambda\epsilon^{(n)}+(1-\lambda)\bar{\epsilon}^{(n-1)} ,\end{aligned} \tag{45}$$

with $\bar{\Phi}^{(0)}=\Phi^{(0)}$ and $\bar{\epsilon}^{(0)}=\epsilon^{(0)}$. The factor λ is chosen optimally to ensure a rapid monotonic convergence of the eigenvalues ϵ_i. After self-consistency has been achieved, temperature is lowered or pressure raised in suitable increments and the iterative procedure is restarted with the previous self-consistent wave functions and energies used in calculating the new matrices $\overleftrightarrow{M}_H$ and $\overleftrightarrow{M}_F$.

V. NUMERICAL RESULTS

We now proceed with the presentation and discussion of results on multilayer physisorption based on a numerical solution of the Hartree-Fock equations (22). The data will include the temperature and pressure dependence of eigenvalues ϵ_i, wave functions Φ_i, adlayer separations, coverage, and coverage-dependent surface potentials. The calculations have been done for several gas-solid systems: ^{3}He-graphite, ^{4}He-graphite, and Ar-Ag.

A. ^{3}He-graphite

The bare surface potential $V_s(z)$ for the helium-graphite system has been studied in detail by Cole *et al.*[2] We adopt the form (32) with the following parameters:

$$\epsilon_s/k_B=16.23\ \text{K},\quad \sigma_s=2.74\ \text{Å} ,$$

$$d_s=3.37\ \text{Å} ,\quad c_s=2,\quad a_s=5.24\ \text{Å} .$$

The parameters of the Lennard-Jones He-He interaction potential (36) are $\epsilon_g/k_B=10.22$ K and $\sigma_g=2.556$ Å. As discussed in Sec. III there is some uncertainty as to the parameter A in (38) that controls the strength of the soft-core repulsion. In this paper we will examine its influence on the

mean-field results by studying two model systems with all potential parameters fixed as above for the ^{3}He-C system but with A chosen so as to get two qualitatively different adsorbate structures. An attempt at a realistic description of the ^{3}He-C system at low coverage will be presented in the next paper of this series where we will fix A by fitted adsorption isotherms, isosteric heat of adsorption, and entropies to experimental data.

We begin with a model ^{3}He-graphite system with $z_0=2.2$ Å, $\alpha=15$,and $A=0.3$ so that $V(z=0)\approx -2V(z=z_{\min})$. We also used a cutoff $q_c^{(j)}=0.58$ Å^{-1} in (30) independent of j to ensure that the maximum adsorbate density is the experimental one of 0.107 atoms/Å^2. We present the discussion of the formation of multilayered mobile ^{3}He physisorbed on graphite in a *Gedanken* experiment in which, starting at high temperatures, we lower the temperature at constant gas pressure, fixed in the following example at $P=1.33$ Pa. At high temperature the Hartree-Fock terms in (22) are negligible due to the smallness of the occupation factors $\tilde{n}_j$. Thus isolated gas particles will find themselves in the bare surface potential $V_s(z)$ which develops five bound states. Lowering the temperature to about 10 K we see in Fig. 2 that the coverage Θ rises to about 0.1 of a monolayer, all adparticles occupying the lowest bound state with energy ϵ_0 which has moved up slightly. At $T\approx 8.5$ K we find that $\epsilon_0=\mu$ and $\Theta\sim 0.4$. The energy ϵ_1 of the first excited state has by now moved up considerably so that its occupation $\tilde{n}_1$ remains negligible. With about half the monolayer volume occupied by gas particles trapped into ϵ_0, the two-body repulsion starts to become important. This causes ϵ_0 to rise substantially as we further lower T to about 6 K at which stage the first monolayer is complete. Most adsorbates including the ^{3}He-C system at low temperature crystallize into a two-dimensional solid before a monolayer is completed. Keeping the ansatz (17) with a momentum cutoff q_c we imply that a summation over the lattice sites in this first monolayer can again be replaced by an integration over a uniform plane of ^{3}He. Using the theory in the Appendix this approximation can readily be improved upon. By now the wave functions of the higher-bound states have been expelled from the immediate vicinity of the surface as evidenced by the average position

$$\langle z_i\rangle=\int z\,|\,\Phi_i(z)\,|^2 dz \tag{46}$$

depicted in the lowest panel of Fig. 2. Additional

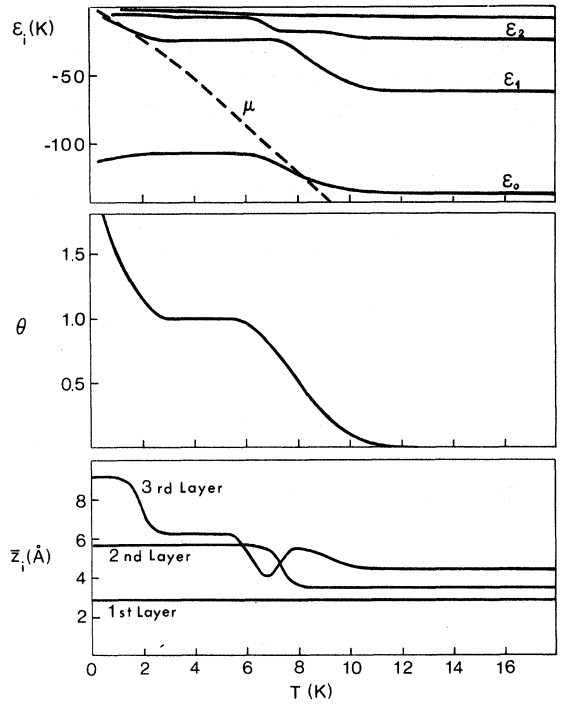

FIG. 2. Single-particle energies ϵ_i from (22), coverage Θ from (26), and mean adlayer positions $\langle z_i\rangle$ from (46) for a model of ^{3}He on graphite for a weakly repulsive two-body interaction (38) with $z_1=2.2$ Å, $A=0.3$, $\alpha=15$ so that $\tilde{V}(0)=-2\tilde{V}(z_{\min})$. $P=1.33$ Pa. For additional parameters see text.

particles approaching from the gas phase now see a new effective surface potential $V_s(z,\Theta=1)$ considerably modified from the bare surface potential depicted in Fig. 3(a) by the mean field $\bar{V}_{\rm MF}(z,\Theta)$ due to the particles already adsorbed in the monolayer, as shown in Fig. 3(b). A definite repulsive barrier appears at $z\approx 4.8$ Å to exclude particles from the region of the filled monolayer. To illustrate this point further we contrast in Figs. 3(a) and 3(b) the lowest three (squared) wave functions at $\Theta=0$ and 1, respectively. Whereas $|\,\Phi_0(z)\,|^2$ remains relatively unchanged, $|\,\Phi_1(z)\,|^2$ changes dramatically, its inner peak having diminished to negligible size and its second one shifted out. Indeed, it appears very much like the new "ground-state" wave function at the position where the second adlayer will eventually form. Lowering the temperature below 3 K we see a similar development to that just described with the ϵ_1 level taking over the role of the lowest bound state energy of interest and the ϵ_2 level representing the first excited state as far as the formation of the second adlayer is concerned. By the time the latter is nearing completion at $T\lesssim 1$ K, $\langle z_3\rangle$ has moved out to about 10.2 Å as

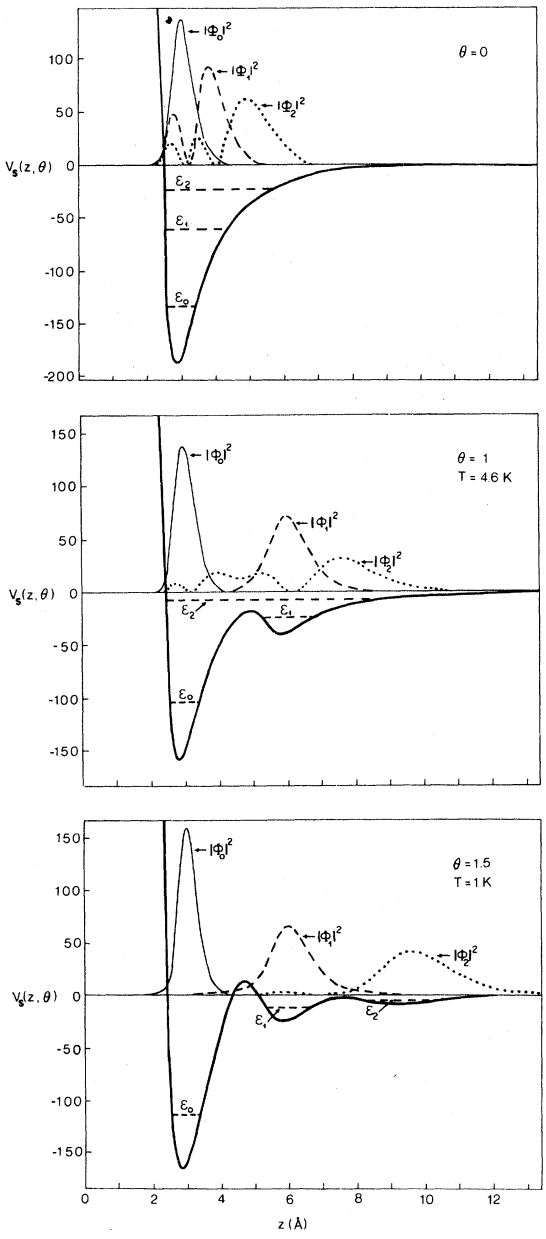

FIG. 3. Effective surface potentials $V_s(z,\Theta)$ from (29) and lowest three squared wave functions for ^{3}He adsorbed on graphite at three different coverages. Parameters as in Fig. 2.

seen in the lower panel of Fig. 2. $|\Phi_1(z)|^2$ has narrowed considerably and the effective surface potential develops three minima for the three adlayers separated by two repulsive barriers, as seen in the lowest panel of Fig. 3. To obtain a complete picture of the development of physisorbed multilayers we have prepared a series of three-dimensional perspective views of the squared wave functions and of the effective coverage-dependent surface potential $V_s(z,\Theta)$ as a function of z and Θ. In Fig. 4 we present a view of $V_s(z,\Theta)$. It is impressive to see how abruptly the repulsive barrier forms in front of the first monolayer as Θ reaches unity. The apparent kink in the bottom of the deepest well closest to the wall is caused by the fact that the coverage-dependent potential shallows slightly with increasing Θ for submonolayer coverage, abruptly stabilizing and leveling off as Θ reaches unity with saturation of the first adsorbed layer; the position of the lowest minimum in $V_s(z,\Theta)$, however, stays fixed at $z_{\min}\approx 2.75$ Å. Figure 5 showing $|\Phi_0(z)|^2$ illustrates through its lack of aberrant features that nothing much happens to the position and shape of the wave function for particles in the first adlayer, the reason being that the bare surface potential $V_s(z)$ is so much stronger and deeper than the mean-field potential arising from the rather weak He-He interaction. Figures 6 and 7 showing several views of $|\Phi_1(z)|^2$ and $|\Phi_2(z)|^2$, respectively, demonstrate very clearly how, as coverage builds up, the higher wave functions move out to form the second and, eventually, the third adlayer. We now also see that the decrease in $\langle z_3 \rangle$ at $T\sim 7$ K in the lowest panel of Fig. 2 is due to a spreading out of $|\Phi_2(z)|^2$ as $|\Phi_1(z)|^2$ moves out.

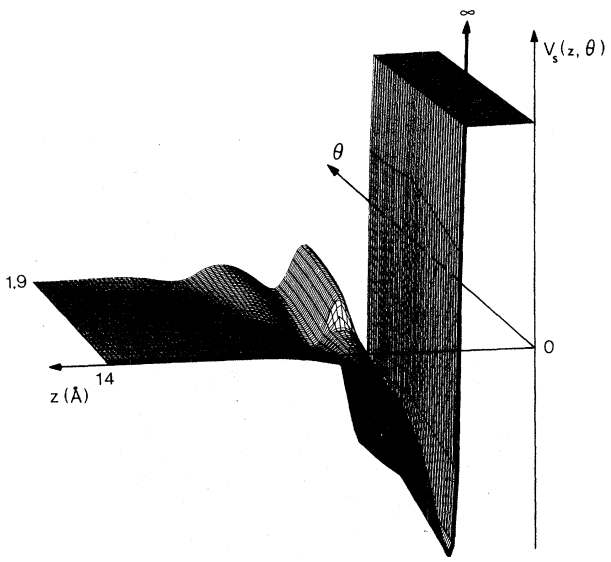

FIG. 4. Perspective view of the effective surface potential $V_s(z,\Theta)$ for ^{3}He on graphite with parameters as in Fig. 2 from (29) plotted over the (z,Θ) plane. For $z\to 0$, $V_s(z,\Theta)\to\infty$. The plateau for small z is used to indicate the distance from the wall.

To illustrate the role in our theory of the parameter determining the height of the soft-core repul-

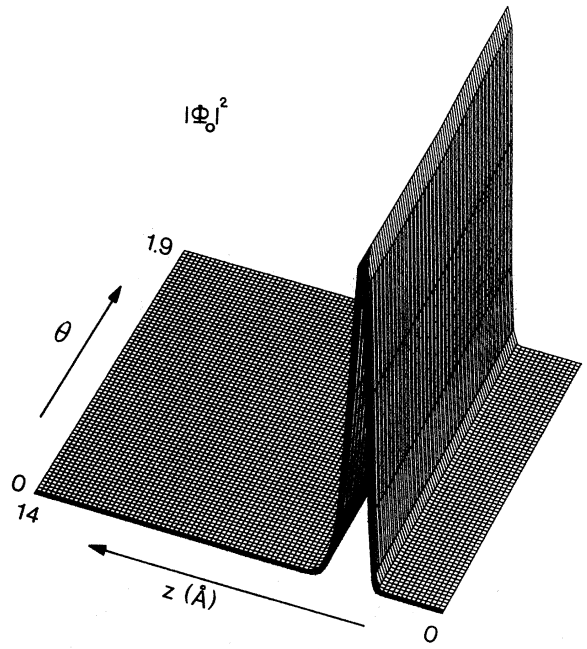

FIG. 5. Perspective view of $|\Phi_0(z)|^2$ over the (z,Θ) plane for ^{3}He on graphite with parameters as in Fig. 2.

sion in $\tilde{V}(z)$ we choose, in a second example, $A=0.048$ so that $\tilde{V}(z=0)\approx -15\tilde{V}(z_{\min})$ substantially higher, by a factor of 7.5, than in the previous model system. Figure 8, which should be compared to Fig. 2, shows the energies ϵ_i, the coverage, and the mean positions $\langle z_i \rangle$ of the lowest three states in the surface potential. Some remarkable qualitative differences can be observed between Figs. 2 and 8. With such a strong repulsion in $\tilde{V}(z)$ the lowest eigenvalue ϵ_0 approaches the chemical potential μ (controlled by the gas phase) around $T\sim 9$ K and then follows it rather closely even after crossing it at $T\sim 3$ K. As a consequence the adsorbate never reaches monolayer coverage down to very low temperatures, so that in this calculation we can remove the cutoff wave number $q_c^{(j)}$ in (30) without affecting the result. Also note that in this example the mean positions $\langle z_i \rangle$ in the lowest panel of Fig. 8 rise monotonically.

In Fig. 9 we present two perspective views of the effective coverage-dependent surface potential $V(z,\Theta)$ as calculated from (29). Note that the repulsive barrier separating the two minima for the first and second adlayer raises smoothly from low coverages and is substantially higher than the one depicted in Fig. 4 for the softer two-body potential $\tilde{V}(z)$. In the present model $|\Phi_0(z)|^2$ looks again

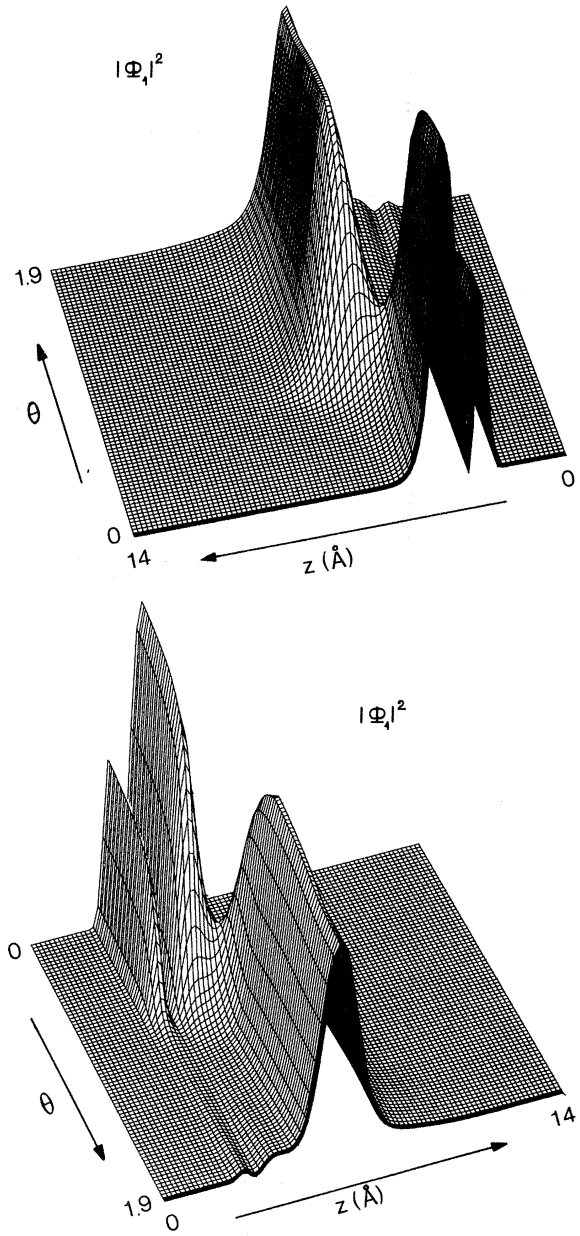

FIG. 6. Perspective views of $|\Phi_1(z)|^2$ over the (z,Θ) plane for ^{3}He on graphite with parameters as in Fig. 2.

very much like Fig. 5. However, $|\Phi_1(z)|^2$ and $|\Phi_2(z)|^2$, shown in Fig. 10, are rather more dramatic than the corresponding Figs. 6 and 7 for the previous example.

So far in our numerical examples we have totally ignored the Brueckner self-consistency requirement in our theory which says that the effective two-body interaction $\tilde{V}(z)$ should be recalculated at each adsorbate density. We have indicated above

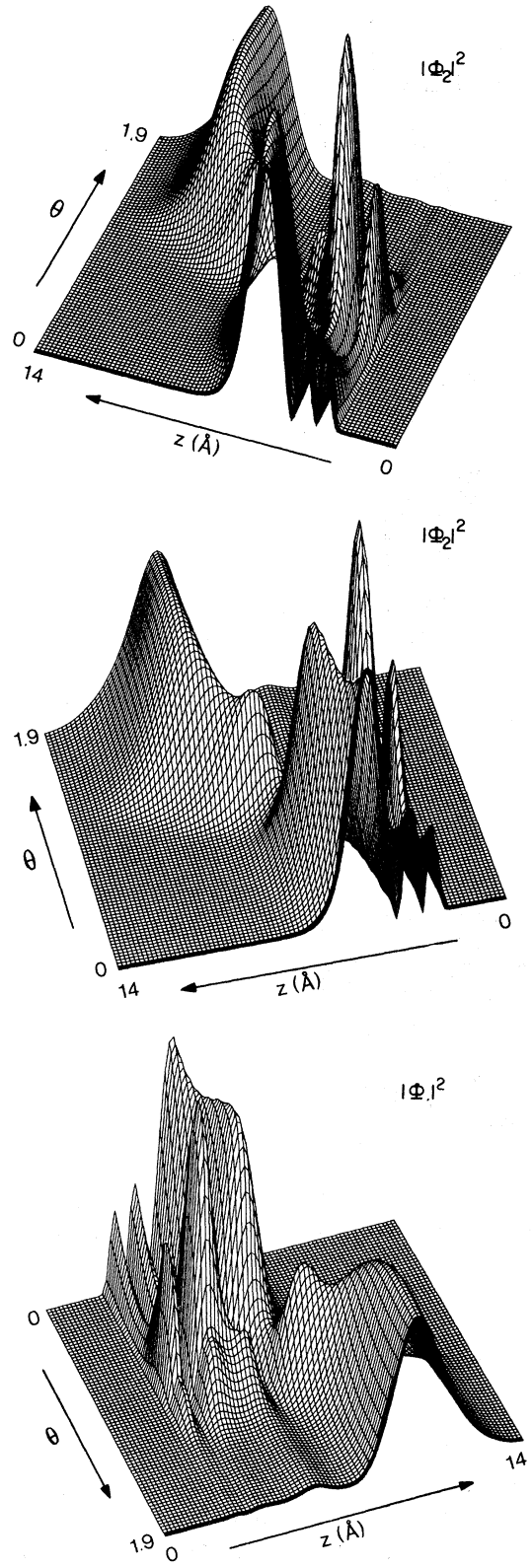

FIG. 7. Perspective views of $|\Phi_2(z)|^2$ over the (z,Θ) plane for ^{3}He on graphite with parameters as in Fig. 2.

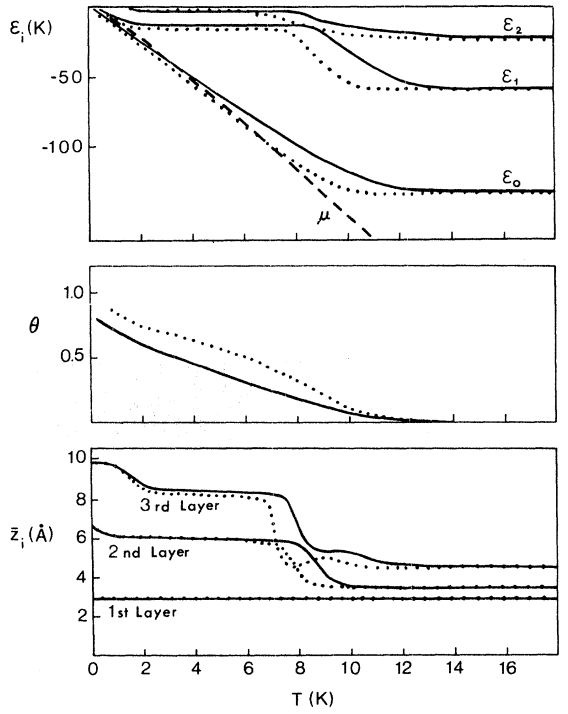

FIG. 8. As Fig. 2 but with $A=0.048$ so that $\tilde{V}(0)=-15\tilde{V}(z_{\min})$ for solid lines. Dotted lines for a model in which $\tilde{V}(0)=0.2\tilde{V}(z_{\min})$ at $\Theta=0$ rising linearly to $\tilde{V}(0)=-15\tilde{V}(z_{\min})$ at $\Theta=1$.

Eq. (37) that a variation of the ^{3}He density does not affect the long-range attractive part of $\tilde{V}(z)$ significantly but causes the repulsion $\tilde{V}(0)$ to increase more or less linearly with density. We have incorporated this dependence into the program by varying $\tilde{V}(0)$ linearly from a value $\tilde{V}(0)=-2\tilde{V}(z_{\min})$ at $\Theta=0$ to $\tilde{V}(0)=-15\tilde{V}(z_{\min})$ at $\Theta=1$. The results are also shown in Fig. 8 as dashed lines. With much less repulsion in particular at small coverages, all curves (energies, coverage, and mean positions) are somewhere between the previous examples.

We have also checked the influence of the exchange term in (22). We found that for a strongly repulsive $\tilde{V}(z=0)$, dropping the exchange term only changes the single-particle energies, the coverage, and the mean positions by a few percent. This justifies *a posteriori* replacing the exponential factor in (18) by unity, and also gives us confidence to do a calculation along similar lines for ^{4}He adsorbing on graphite.

The two model systems studied so far have been chosen to demonstrate the range of qualitatively different adsorbate structures as they are calculated in mean field theory. To find a realistic descrip-

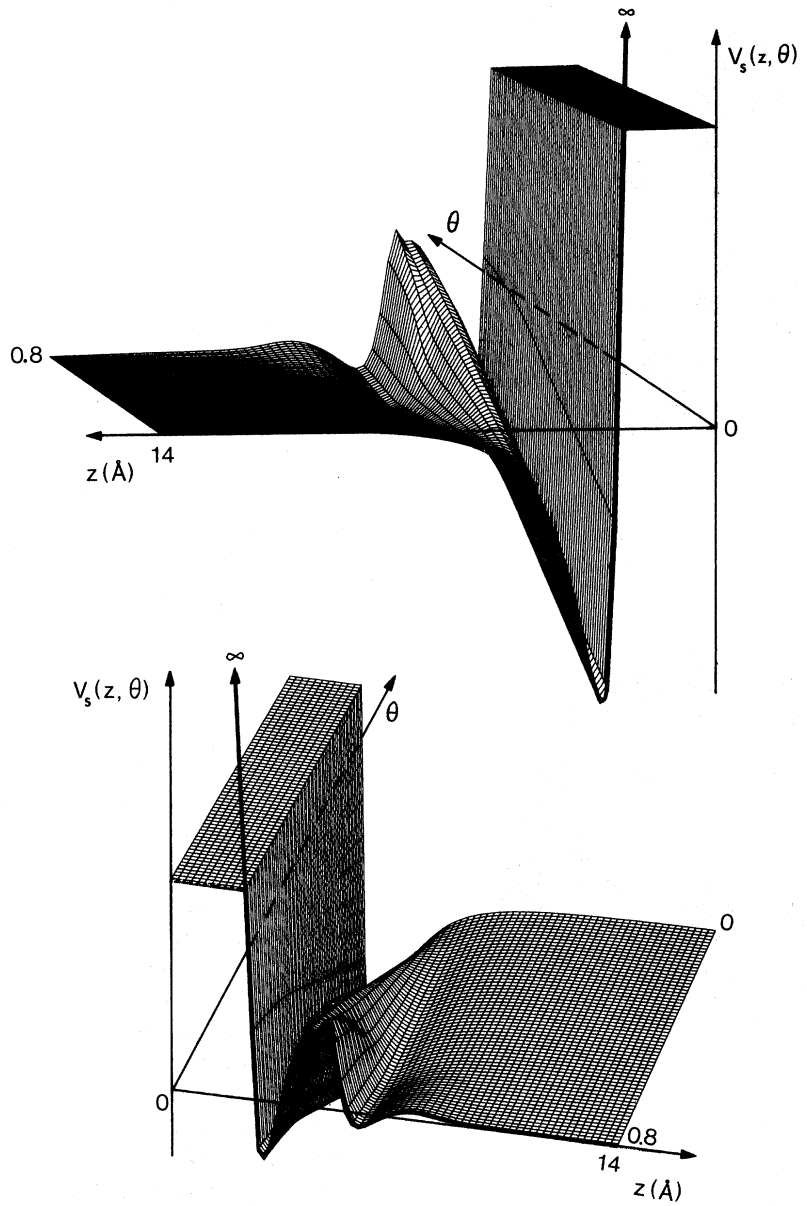

FIG. 9. Two perspective views of the effective coverage-dependent surface potential (29) over the (z,Θ) plane for ^{3}He on graphite with the parameters of Fig. 8.

tion of the ^{3}He-C system we plan to calculate in the next paper of this series various thermodynamic functions such as the adsorption isotherm, the heat of adsorption, etc. A fit to experimental data will then fix the parameter A in (38) for submonolayer fluid adsorbates. Indeed, our calculations indicate that the effective potential as calculated from Brueckner's theory and illustrated in Fig. 1 is quite appropriate.

B. ^{4}He-graphite

We have performed a calculation for a model Bose gas (^{4}He) adsorbing on graphite using the effective interaction (38) between ^{4}He atoms and adjusting the height of the repulsive barrier so that $\tilde{V}(z=0)=-0.2\tilde{V}(z_{\min})$ for $\Theta=0$ increasing to $\tilde{V}(z=0)=-15\tilde{V}(z_{\min})$ for $\Theta=1$. This is the same

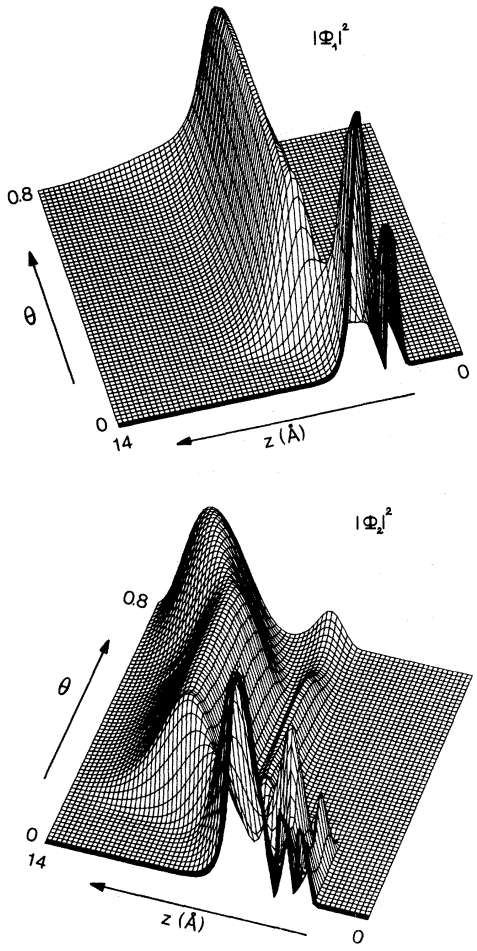

FIG. 10. Perspective views of $|\Phi_1(z)|^2$ and $|\Phi_2(z)|^2$ over the (z,Θ) plane for ^{3}He on graphite with the parameters of Figs. 8 and 9.

two-body interaction that leads for the model ^{3}He-graphite system to the set of dashed curves in Fig. 8. For the model Bose system the results are summarized in Fig. 11. Compared to the fermionic (^{3}He-graphite) system in Fig. 8 energies ϵ_i and mean adlayer positions $\langle z_i \rangle$ vary much more smoothly. In particular, note that all ϵ_i's must remain larger than μ to keep the Bose-Einstein occupation functions from becoming infinite. This is in contrast to adsorbing fermionic gas particles for which the ϵ_i's must actually cross the chemical potential to get monolayer completion (see Fig. 2). This qualitative difference indeed shows up between the ^{3}He-graphite and ^{4}He-graphite systems resulting in a different behavior of isosteric heat of adsorption, isotherms, and the specific-heat contribution from the excited states. For heavier adsorbate particles, on the other hand, the repulsion in

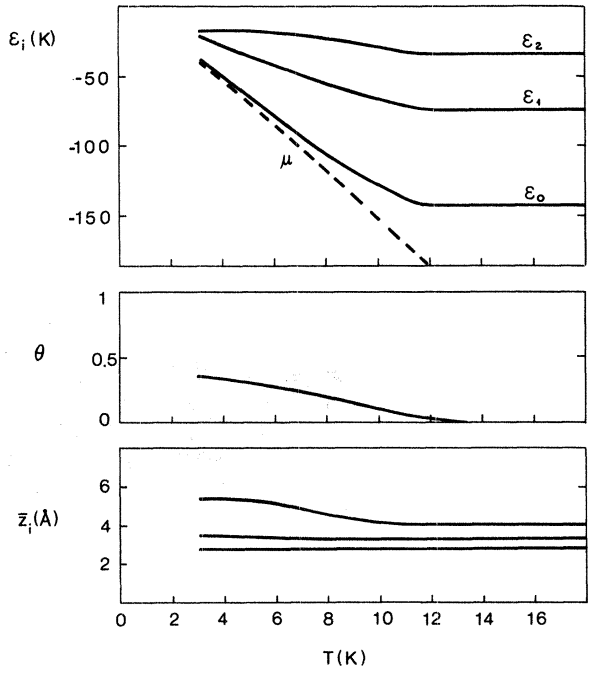

FIG. 11. Single-particle energies ϵ_i from (22), coverage Θ from (26), and mean adlayer positions $\langle z_i \rangle$ from (46) for a model of ^{4}He on graphite with a strongly repulsive two-body interaction (38) with $z_1 = 2.2$ Å, $A = 0.048$, $\alpha = 15$ so that $\tilde{V}(0) = -15\tilde{V}(z_{\min})$. $P = 1.33$ Pa. For additional parameters see text.

$\tilde{V}(z)$ must be relatively large so that fermionic and bosonic gas particles behave more alike, compare Figs. 8 and 11 for model calculations.

Figures 12 and 13 show perspective views of the coverage-dependent surface potential $V_s(z,\Theta)$ and of the (squared) wave functions $|\Phi_1(z)|^2$ and $|\Phi_2(z)|^2$, respectively, for the parameters of Fig. 11. They should be compared to Figs. 9 and 10 for the model ^{3}He-graphite system. Again a fit to experimental data on thermodynamic functions of the ^{4}He-C system will determine the parameter A. This will be reported elsewhere.

C. Argon on silver

As a last example we study the adsorption of argon on silver. For the bare surface potential we choose the Morse potential (34) with the following parameters: $U_0/k_B = 430$ K, $\gamma_s^{-1} = 0.59$ Å, and $z_0 = 0.59$ Å. The bare Ar-Ar interaction we assume to be a Lennard-Jones potential (36) with $\epsilon_g/k_B = 119.8$ K and $\sigma_g = 3.05$ Å. In addition, to specify the effective one-dimensional soft-core po-

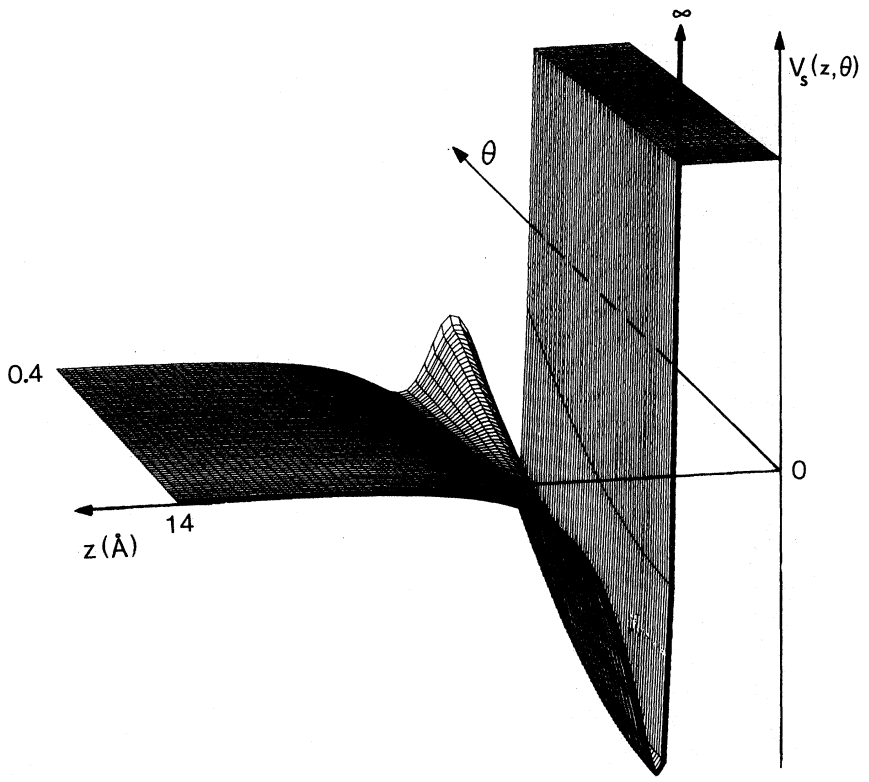

FIG. 12. See Fig. 4. Parameters as in Fig. 11.

tential (38) we choose $z_1=2.84$ Å, $\alpha=15$, and $A=0.15$ so that $\tilde{V}(0)\approx -5\tilde{V}(z_{\min})$. Note that the range of the Ar-Ar interaction is much larger than the range of the bare surface potential, in constrast to the He-graphite system. In Fig. 14 we present the numerical results on the single-particle energies, the coverage, and the mean positions of the lowest three states as a function of temperature. Our iterative method of solving the Hartree-Fock equations only works up to a coverage of about 0.35. We find this quite satisfactory as argon will quite likely not form a mobile fluid adsorbate for much greater coverages. What is, indeed, even more gratifying is the fact that the curves in Fig. 14 are the same within a few percent whether we do the calculations for Ar obeying Bose-Einstein statistics or Fermi-Dirac statistics.

Because the range of the Ar-Ar interaction is so much larger than the range of the Ar-Ag surface potential, the second adlayer will form very far from the surface as evidenced by the increase of $\langle z_2 \rangle$ from 0.68 Å to 4.2 Å for $T<15$ K. This feature is further dramatically illustrated in the behavior of the wave functions in Fig. 15. The effective coverage-dependent surface potential for the Ar-Ag system is finally given in Fig. 16.

VI. CONCLUDING REMARKS

We have developed a mean-field theory for the physisorption of a mobile fluid adsorbate on a solid surface for non-negligible coverages where atom-atom interactions within the adsorbate become important. A reduction to a one-dimensional problem and a few controllable approximations have allowed us to derive Hartree-Fock equations that can be solved numerically. In this paper we have looked at some model systems and studied the dependence of binding energies and wave functions of the adsorbed particles on temperature, pressure and thus on coverage. Adlayer positions were calculated and an effective coverage-dependent surface potential was determined. In the following paper we intend to study the thermodynamics of the adsorbate in realistic models for the ^{3}He-C and ^{4}He-C systems by calculating from our mean-field theory, adsorption isotherms, isosteric heats of adsorption, differential entropies, and specific heats. A third paper of this series is planned to be devoted to the adsorption and desorption kinetics, for which we will develop a master equation approach extending the theory of Refs. 9 and 10 to non-negligible coverages. One of the new features that

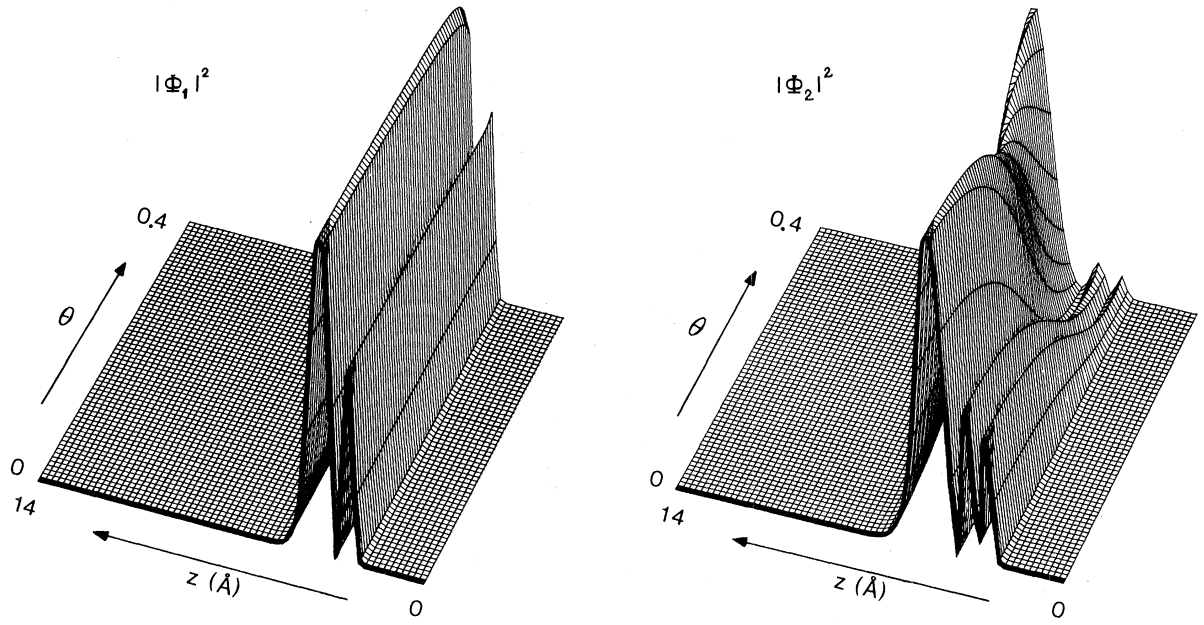

FIG. 13. Perspective views of wavefunctions $|\Phi_1(z)|^2$ and $|\Phi_2(z)|^2$ of first two excited states for the parameters of Fig. 11.

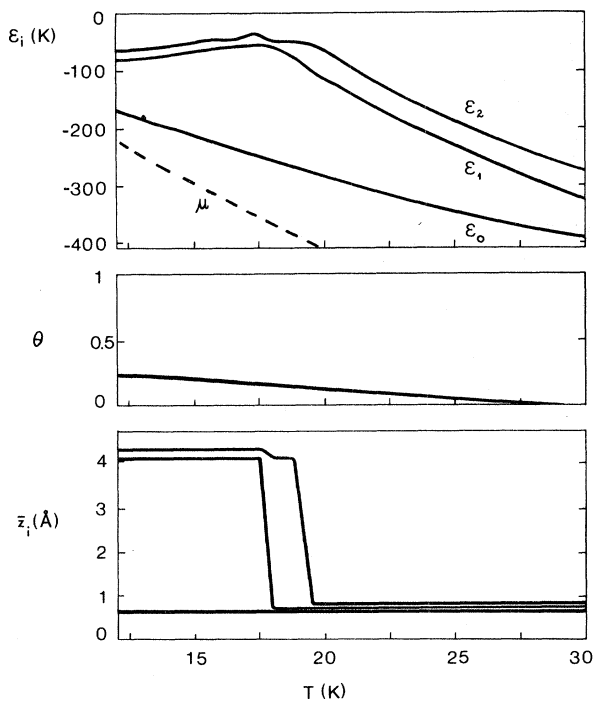

FIG. 14. Single-particle energies ϵ_i from (22), coverage Θ from (26) and mean adlayer positions $\langle z_i \rangle$ from (46) for a model of Ar on Ag. For potential parameters see text.

will emerge arises from the fact that for $\Theta \lesssim 1$ the effective surface potential develops a confining barrier in front of the first adlayer (illustrated, e.g., in Figs. 3, 4, 9, 12, and 16) so that desorption from an adsorbate with $\Theta \sim 1$ will become an activated process.

ACKNOWLEDGMENT

This work was supported in part by the Natural Sciences and Engineering Research Council of Canada.

APPENDIX

In this appendix we show how to reduce the Hartree-Fock equations (15) to a one-dimensional problem for gas-solid systems for which the periodicity of the surface potential $V_s(\vec{r})$ or of the adsorbate along the surface is essential. We write

$$V_s(\vec{r}) = V_s(\vec{\rho},z) = \frac{N_s}{L^2} \sum_n v_s(\vec{\rho}-\vec{\rho}_n,z) , \qquad \text{(A1)}$$

where N_s is the number of atoms at positions $\vec{\rho}_n$ in the surface of area L^2. Periodicity of v_s implies that

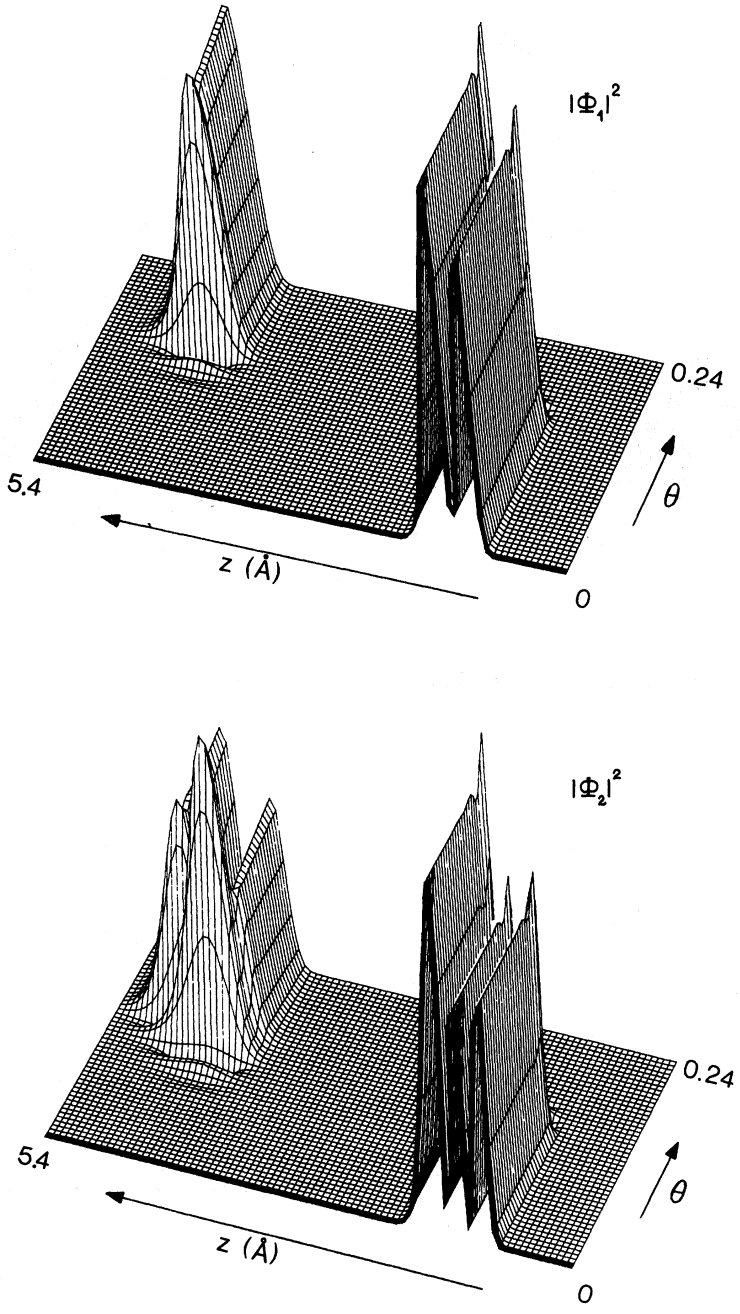

FIG. 15. Wave functions $|\Phi_1(z)|^2$ and $|\Phi_2(z)|^2$ of first two excited states for the parameters of Fig. 14.

$$V_s(\vec{\rho}+\vec{\rho}_m,z)=V_s(\vec{\rho},z)\ . \tag{A2}$$

Instead of (17) we write

$$\psi_{\vec{i}}(\vec{r})=\psi_{i\vec{q}}(\vec{\rho},z)=L^{-1}e^{i\vec{q}\cdot\vec{\rho}}u_{i\vec{q}}(\vec{\rho},z)\ , \tag{A3}$$

where

$$u_{i\vec{q}}(\vec{\rho}+\vec{\rho}_m,z)=u_{i\vec{q}}(\vec{\rho},z) \tag{A4}$$

is periodic.

We expand V_s and $\psi_{\vec{i}}$ in Fourier series in inverse two-dimensional lattice vectors $\vec{g}$,

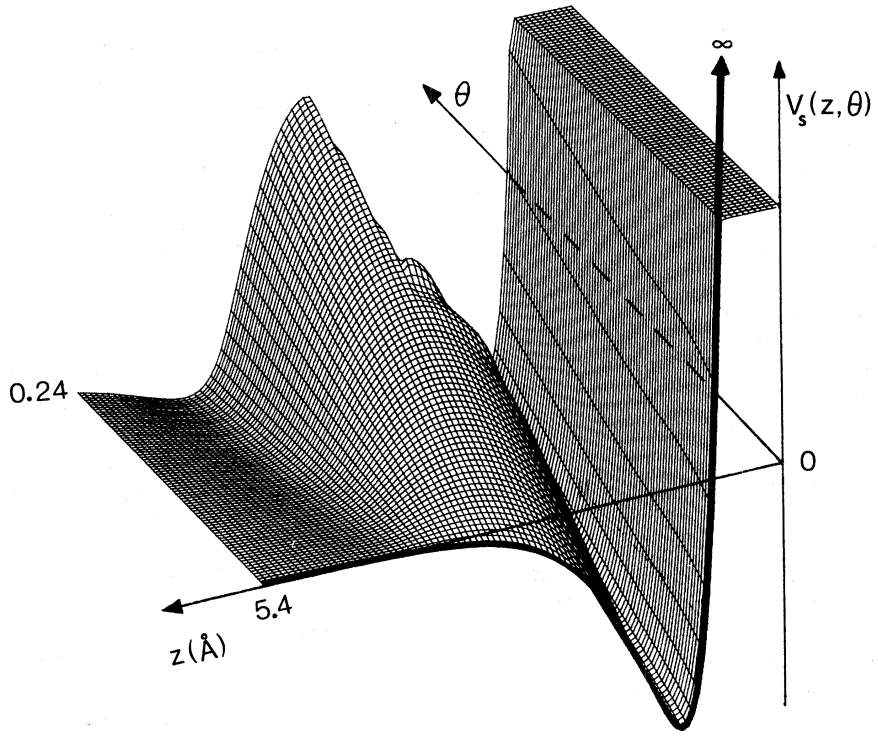

FIG. 16. Effective coverage-dependent surface potential for Ar-Ag.

$$V_s(\vec{\rho},z)=\sum_{\vec{g}} e^{i\vec{g}\cdot\vec{\rho}}\tilde{V}^s_{\vec{g}}(z) \tag{A5}$$

and

$$\psi_i(\vec{\rho},z)=L^{-1}e^{i\vec{q}\cdot\vec{\rho}}\sum_{\vec{g}} e^{i\vec{g}\cdot\vec{\rho}}\tilde{u}_{i,\vec{g}}(\vec{q},z) \tag{A6}$$

and insert (A5) and (A6) into (15). Multiplying with appropriate factors $\exp(i\vec{g}'\cdot\vec{\rho})$ and integrating over $\vec{\rho}$, we obtain after some algebra

$$\left[-\frac{\hbar^2}{2m}\frac{d^2}{dz_1^2}+\epsilon_{i\vec{g}}(\vec{q}_i)\right]\tilde{u}_{i\vec{g}}(\vec{q}_i,z_1)+\sum_{\vec{g}_1}\tilde{V}^s_{\vec{g}_1}(z_1)\tilde{u}_{i\vec{g}-\vec{g}_1}(\vec{q}_i,z_1)$$
$$+L^{-2}\sum_{\vec{g}_1\vec{g}_3}\sum_{j\vec{q}_j} n_j(\vec{q}_j)\left[(2s+1)\int_0^\infty dz_2\tilde{u}_{j\vec{g}_1}(\vec{q}_j,z_2)W_2(\vec{g}_3-\vec{g}_1,z_{12})\,\tilde{u}_{j\vec{g}_3}(\vec{q}_j,z_2)\tilde{u}_{i,\vec{g}+\vec{g}_1-\vec{g}_3}(\vec{q}_i,z_1)\right.$$
$$-\int_0^\infty dz_2\tilde{u}_{j\vec{g}_1}(\vec{q}_j,z_2)W_2(\vec{q}_i-\vec{q}_j+\vec{g}_3-\vec{g}_1,z_{12})$$
$$\left.\times\tilde{u}_{i\vec{g}_3}(\vec{q}_i,z_{12})\tilde{u}_{j,\vec{g}+\vec{g}_1-\vec{g}_3}(\vec{q}_j,z_1)\right]=0\,. \tag{A7}$$

where

$$W_{\rm eff}(\vec{Q},z)=\int d\vec{\rho}e^{i\vec{Q}\cdot\vec{\rho}}V_{\rm eff}(\vec{\rho},z) \tag{A8}$$

is the two-dimensional Fourier transform of the effective two-body interaction between the gas particles and

$$\epsilon_i(\vec{Q})=E_{\vec{i}}-\frac{\hbar^2}{2m}Q^2\,. \tag{A9}$$

Note that even for a uniform surface potential $V_s(\vec{\rho},z)=\tilde{V}_0(z)$, (A7) with $\vec{g}_1=0$ still allows the adsorbate to form a lattice due to the two-body interaction. We recover Eqs. (18) for a uniform adsorbate from (A7) by setting all inverse lattice vectors equal to zero.

*On leave of absence from Marii-Curie-Sklodowska University, Lublin, Poland.

[1]W. A. Steele, *Interaction of Gases with Solid Surfaces* (Pergamon, Oxford, 1974).

[2]For the He-graphite system $V_s(\vec{r})$ has been analyzed in detail by W. E. Carlos and M. W. Cole, Phys. Rev. Lett. 49, 697 (1979); G. Vidali and M. W. Cole, Phys. Rev. B 22, 4661 (1980). See also a recent review by M. W. Cole, D. R. Frankl, and D. L. Goodstein, Rev. Mod. Phys. 53, 199 (1981).

[3]For a review see, e.g., J. G. Dash and M. Schick, in *The Physics of Liquid and Solid Helium, Part II,* edited by K. H. Bennemann and J. B. Ketterson (Wiley, New York, 1978).

[4]See also Chia-Wei Woo, in *The Physics of Liquid and Solid Helium, Part I,* edited by K. H. Bennemann and J. B. Ketterson (Wiley, New York, 1978).

[5]A. D. Navaco, Phys. Rev. A 7, 1653 (1973).

[6]The quantum statistical theory of phonon-mediated desorption was developed by J. E. Lennard-Jones and C. Strachan, Proc. R. Soc. London Ser. A 150, 442 (1935); J. E. Lennard-Jones and A. Devonshire, *ibid.* 156, 6 (1936); 156, 29 (1936).

[7]Z. W. Gortel and H. J. Kreuzer, Chem. Phys. Lett. 67, 197 (1979); Z. W. Gortel, H. J. Kreuzer, and D. Spaner, J. Chem. Phys. 72, 234 (1980); Z. W. Gortel, H. J. Kreuzer, and R. Teshima, Can. J. Phys. 58, 376 (1980).

[8]Z. W. Gortel, H. J. Kreuzer, and R. Teshima, Phys. Rev. B 22, 512 (1980).

[9]Z. W. Gortel, H. Z. Kreuzer, and R. Teshima, Phys. Rev. B 22, 5655 (1980).

[10]Z. W. Gortel, H. J. Kreuzer, R. Teshima, and L. A. Turski, Phys. Rev. B 24, 4456 (1981); H. J. Kreuzer and R. Teshima, *ibid.* 24, 4470 (1981).

[11]Such an approach has been pursued now for over 20 years by the Hartree-Fock practitioners for finite nuclei. For a review see, e.g., J. P. Svenne, Adv. Nucl. Phys. 11, 179 (1979).

[12]K. A. Brueckner, J. L. Gammel, and H. Weitzner, Phys. Rev. 110, 431 (1958).

[13]See, e.g., E. Østgaard, Phys. Rev. 168, 1139 (1968).

[14]The zero temperature Brueckner-Hartree-Fock equations are given in Ref. 12. The extension to finite temperatures follows the arguments developed for Hartree-Fock theory; see, e.g., A. L. Fetter and J. D. Walecka, *Quantum Theory of Many-Particle Systems* (McGraw-Hill, New York, 1971). Also note that a variational term $\delta K/\delta\psi$ has been dropped in arriving at (7); for a justification see, e.g., B. H. Bandow, Ann. Phys. (N.Y.) 74, 112 (1972).

[15]See, e.g., E. Østgaard, Phys. Rev. 170, 257 (1968).

[16]The situation is somewhat easier in nuclear structure calculations where the spherical symmetry of finite nuclei allows further simplifications of (7).

[17]This effective potential can be further approximated as $V_{\text{eff}}(\vec{r}) \approx V_2(r)u_0(\bar{k},r)/\sin(\bar{k}r)$ with little dependence on $\bar{k}$. This form has been introduced in Ref. 12. Numerical examples for liquid ^{3}He are given, also for higher partial waves, in Ref. 15.

[18]J. C. Slater, Phys. Rev. 81, 385 (1951).

[19]H. B. Ghassib, R. H. Ibarra, and J. M. Irvine, Ann. Phys. (N.Y.) 85, 378 (1974).